Parametric forcing of waves with a nonmonotonic dispersion relation: Domain structures in ferrofluids

David Raitt
SCRI, Florida State University B-186, 400 Dirac Science Center Library, Tallahassee, Florida 32306

Hermann Riecke
Department of Engineering Sciences and Applied Mathematics, Northwestern University, Evanston, Illinois 60208

(Received 22 January 1996)

Surface waves on ferrofluids exposed to a dc magnetic field exhibit a nonmonotonic dispersion relation. The effect of a parametric driving on such waves is studied within suitable coupled Ginzburg-Landau equations. Due to the nonmonotonicity the neutral curve for the excitation of standing waves can have up to three minima. The stability of the waves with respect to long-wave perturbations is determined *via* a phase-diffusion equation. It shows that the band of stable wave numbers can split up into two or three subbands. The resulting competition between the wave numbers corresponding to the respective subbands leads quite naturally to patterns consisting of multiple domains of standing waves which differ in their wave number. The coarsening dynamics of such domain structures is addressed. [S1063-651X(97)12201-2]

PACS number(s): 47.20.−k, 05.45.+b, 05.90.+m

I. INTRODUCTION

Spatial patterns have been studied extensively over the past years, the classic examples being Rayleigh-Bénard convection, Taylor vortex flow, and structures arising in directional solidification [1]. It has been well established that long-wavelength perturbations of such steady patterns exhibit diffusive phase dynamics [2] with the phase-diffusion coefficient changing sign at the Eckhaus instability [3,4]. Thus, after the decay of transients, one-dimensional steady patterns usually relax to a strictly periodic pattern.

It has been pointed out, however, that this need not be the case in general; there are situations in which the final state consists of a number of domains with different wave numbers [5–9]. This can occur if the phase-diffusion coefficient becomes negative such that the band of stable wave numbers is split into two parts. Within each domain the wave number is then in one of the two stable subbands. Experimentally, such domain structures have been observed in Rayleigh-Bénard convection in a narrow channel [10]. However, so far it has not been firmly established whether the origin of these states is in fact due to a splitting of the stable band since the phase-diffusion coefficient has not been measured in this regime. From a theoretical point of view this experiment is difficult to analyze, since the domain structures arise only at very large Rayleigh numbers which require full numerical simulations of the three-dimensional Navier-Stokes equations.

Very recently, two-dimensional domain structures have been observed in experiments on optical beams in a ring cavity [11]. In certain parameter regimes the light intensity in the cross section of the beam was found to exhibit coexisting stripes and hexagonal patterns with clearly distinct wave numbers. The precise origin of these domain structures has not yet been established.

Domain structures can be viewed as arising from the competition between different wave numbers. For their investigation it is therefore natural to turn to pattern-forming systems which have a neutral curve, with two or more minima corresponding to the competing wave numbers. Domain structures are then expected to arise close to threshold, where they may be described analytically within a small-amplitude theory [6,9,12,13]. In addition, in this regime interesting locking [14] and coarsening phenomena are possible which are not expected at large amplitudes [12,13,15–17].

So far, not many physical systems have been identified which exhibit a neutral curve with two minima. Note that within the framework of Ginzburg-Landau equations it is not sufficient if two different modes with different wave numbers go unstable at the same value of the control parameter. Since the stability of the domain structures relies either on phase conservation [8,6,13] or on a locking-in of interacting fronts [13] (see also below), both minima have to correspond to the same mode.

For traveling waves a neutral curve with a double minimum has recently been identified in convection of a conducting fluid in a rotating annulus in the presence of a magnetic field [18]. This system is, however, not easily accessible in experiments.

In this paper we show that neutral curves with multiple minima, and the resulting domain structures, may be obtained quite naturally by a parametric driving of waves with *nonmonotonic* dispersion relation. Then there exists a range of frequencies in which modes with different wave numbers resonate simultaneously with the driving. The dispersion relation becomes nonmonotonic when the group velocity changes sign. This is the case in spiral vortex flow between counter-rotating cylinders in certain parameter regimes [19]. However, the parametric forcing of spiral vortex flow has turned out to be nontrivial due to the appearance of Stokes layers [20]. If the parametric driving can be applied *via* a bulk forcing (e.g., using electric or magnetic fields) its effect is considerably stronger. For instance, standing waves are excited very efficiently by an ac electric field in electrohydrodynamic convection in nematic liquid crystals [21,22]. This suggests considering the effect of an ac magnetic field on surface waves on ferrofluids. They exhibit a nonmonotonic dispersion relation if they are exposed to a sufficiently

strong dc magnetic field [23]. In fact, the nonmonotonicity is a precursor of the Rosensweig instability [24,25]. Quite analogously, surface waves on conducting and dielectric fluids in the presence of an electric field exhibit a nonmonotonic dispersion relation leading to an instability for larger fields [26–29].

The organization of the paper is as follows. To describe parametrically driven waves for small amplitudes, in Sec. II we introduce in suitable coupled complex Ginzburg-Landau equations. In Sec. III we study analytically the long-wave stability of standing waves which are parametrically excited by a periodic forcing (e.g., by an ac magnetic or ac electric field). In the expected parameter regime the band of stable wave numbers separates into three subbands. The numerical simulations presented in Sec. IV confirm the existence and stability of structures consisting of domains with different wave number. In addition, we present numerical results for the coarsening of arrays of domains within a single, fourth-order Ginzburg-Landau equation which can be derived from the coupled Ginzburg-Landau equations under suitable conditions.

II. MODEL

For small amplitudes and small damping parametrically driven waves can be described by coupled Ginzburg-Landau equations [30–32]. A crucial ingredient for determining the linear part of these equations is the dispersion relation of the waves. For surface waves on an inviscid ferrofluid of infinite depth in the presence of a dc magnetic field, it is given by [24]

$$\omega^2(q)=gq+\frac{\sigma}{\rho}q^3-\frac{1}{\rho(1/\mu_0+1/\mu)}M_0^2q^2. \tag{1}$$

Here g is the gravitational acceleration, σ the surface tension, ρ the density of the fluid, μ the permeability, and M_0 the magnetization of the fluid. When M_0^2 is increased beyond $M_c^2\equiv\sqrt{3g\sigma\rho}(1/\mu_0+1/\mu)$ the dispersion relation becomes nonmonotonic and is given by a cubic polynomial in the vicinity of the inflection point. To capture this cubic dispersion relation third spatial derivatives are retained in the Ginzburg-Landau equations,

$$\partial_t A+v\,\partial_x A=d\,\partial_x^2 A+f\,\partial_x^3 A+aA+bB+cA|A|^2 +(n-c)|B|^2A, \tag{2}$$

$$\partial_t B-v\,\partial_x B=d^*\partial_x^2 B+f^*\partial_x^3 B+a^*B+bA+c^*B|B|^2 +(n^*-c^*)|B|^2B. \tag{3}$$

Physical quantities like the surface height h are described in terms of the complex amplitudes as

$$h=\delta e^{iq_0\hat{x}}(A(x,t)e^{-\omega_e/2\hat{t}}+B(x,t)e^{\omega_e/2\hat{t}})+\text{c.c.}+\text{h.o.t.},\quad \delta\ll 1, \tag{4}$$

where the amplitudes A and B depend on slow space and time coordinates, $t=\delta^2\hat{t}$, $x=\delta\hat{x}$, and h.o.t. stands for higher-order terms. The parametric driving, which can be achieved with an additional ac magnetic field, enters the equations *via* the linear coupling terms bA and bB, respectively. Its strength is proportional to the coefficient b [30,31], which can be chosen real. All other coefficients are in general complex. The second control parameter is the detuning between the frequency ω_e of the external driving and the natural frequency ω_0 of waves with wave number q_0, $\omega_0=\omega_e/2+a_i-\alpha a_r$ with α being an $O(1)$ quantity and $a\equiv a_r+ia_i$. The carrier wave number q_0 is chosen to be that wave number for which the dispersion relation (1) has an inflection point with zero slope. This occurs for $M_0=M_c$. At this point the linear group velocity v_r and as the quadratic dispersion term d_i vanish. As long as M_0 is close to M_c these dispersive terms are therefore small, and it is consistent to keep also the third-order term which gives the cubic dispersion relation. In all of the following we assume that the viscosity of the fluid is low. The dissipative terms are then small with the leading order term being a_r, allowing us to neglect the imaginary part of f. However, we keep v_i and d_r, which give the linear and quadratic dependence of the damping on the wave number, although they are also of higher order than a_r. In this paper we do not attempt to

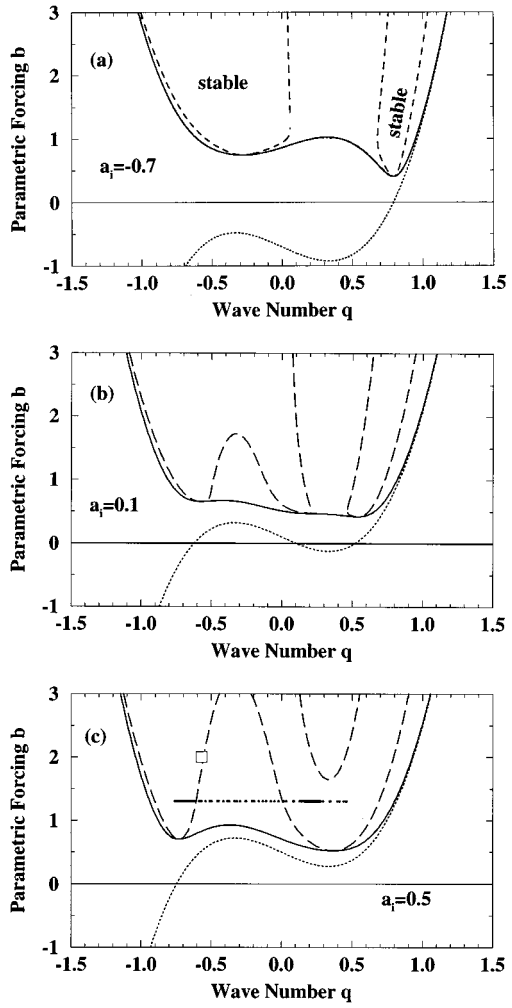

FIG. 1. The neutral-stability (solid line) and Eckhaus (dashed line) curves for Eqs. (2) and (3) for $a_r=-0.5$, $d=0.1$, $v=1+0.2i$, $c=-1-0.5i$, $n=-3+2i$, $f=-3$, and various values of the detuning a_i as indicated. The dotted line in (c) indicates the wave-number distribution of the structure shown in Fig. 2.

make quantitative predictions for a specific experimental system. Therefore we do not calculate the coefficients of Eqs. (2) and (3). Instead we present results that should be typical of the parametric driving of waves with the nonmonotonic dispersion relation.

The neutral-stability curve, at which the basic state (with flat surface) becomes unstable, is given by

$$b^2=|R|^2 \quad \text{with} \quad R=a-ivq-dq^2-ifq^3. \tag{5}$$

The resulting neutral-stability curve is sixth order in q, and can therefore have up to three minima. Depending on the parameters, the absolute minimum of the neutral-stability curve can be any one of the three. Of course, the situation with a single minimum can be recovered as well. Examples of neutral curves with multiple minima are given by the solid lines in Figs. 1(a)–1(c). There the effect of changing the driving frequency, i.e., the detuning a_i, is demonstrated. The difference between half the external frequency and the frequency of a wave with wave number q is indicated by the dotted line. The damping is also taken to be wave number dependent (v_i and d_r nonzero). As expected, the neutral curve exhibits local minima at the resonance wave numbers. As the detuning is changed from negative to positive values, the absolute minimum shifts from the resonance at high wave number to that at low wave number.

It should be noted that neutral curves with double minima can also be obtained if the dispersion relation has a *single* extremum. Near that extremem v_r is small but d_i is not, and small-amplitude waves can be described using Eqs. (2) and (3) without the third-derivative term [6].

III. LINEAR STABILITY AND PHASE DIFFUSION

The multiple wells in the neutral curve suggest that the band of stable wave numbers also splits into separate subbands. This is a prerequisite for stable domain structures to exist. We therefore determine the linear stability of the nonlinear waves with respect to long-wave perturbations. This is done most efficiently by deriving the phase-diffusion equation [2,6]

$$\partial_T\phi(X,T)=\mathcal{D}(q)\partial_X^2\phi(X,T). \tag{6}$$

In this description the amplitudes A and B are proportional to $S(q)e^{i\phi/\epsilon}+O(\epsilon)$, where the amplitude S of the wave satisfies

$$b^2=|n|^2S^4+2n^*RS^2+|R|^2, \tag{7}$$

and $X=\epsilon x$ and $T=\epsilon^2 t$ are superslow scales. The phase ϕ gives the local wave number via $q=\partial_X\phi$. In order to simplify the expression for $\mathcal{D}(q)$, the following notation is introduced:

$$a*b=a_rb_r+a_ib_i, \quad a\bullet b=a_rb_i+a_ib_r \tag{8}$$

The phase diffusion coefficient $\mathcal{D}(q)$ can then be written as $D(q)/\tau(q)$ with

$$\begin{aligned}D(q)=&-\{4(3c_ifq+c^*d)|n|^2\}S^6-\{-18c*n^*f^2q^4+24(\mathrm{Im}(d^*cn))fq^3+[-12(\mathrm{Re}(v^*cn))f\\&+8(d*d^*c*n^*+2d_rd_ic\bullet n)]q^2+[6(R_i|n|^2+2c_in^*R)f+8(\mathrm{Im}(cd^*nv^*))]q+2[d^*R|n|^2+2n^*Rc^*d\\&-v*v^*c*n^*-2v_rv_ic\bullet n]\}S^4-\{9[-R*n^*+2R_ic_i]f^2q^4+12[c_id_rR_r+(c_id_i+c*d)R_i+\mathrm{Im}(Rnd^*)]fq^3\\&+[6(-c_iv_iR_r+(c_iv_r+c\bullet v^*)R_i-\mathrm{Re}(Rnv^*))f+8c*dd*R+4d*d^*n*R^*+8d_rd_in\bullet R]q^2+[4(v^*\bullet Rd*n\\&+v*Rd^*\bullet n+c*dv^*\bullet R+d*Rv^*\bullet c)+6R_ifn*R]q+[2(d_rn_rR_r^2+d_in_iR_i^2+d\bullet nR_rR_i)-2(c+n)\bullet Rv_rv_i\\&+(2c_iR_i-n*R^*)v_r^2+(2c_rR_r+n*R^*)v_i^2]\}S^2-\{9R_i^2f^2q^4+12d*RR_ifq^3+[6R\bullet v^*R_if+4(d*R)^2]q^2\\&+4d*RR\bullet v^*q+(R\bullet v^*)^2\}\end{aligned} \tag{9}$$

and

$$\tau(q)=-4c_r|n|^2S^6-(4c_rn^*R+2R_r|n|^2)S^4-2R_rn^*RS^2. \tag{10}$$

Here $\mathrm{Re}(a)$ and $\mathrm{Im}(a)$ denote the real and imaginary part of a, respectively.

The stability limit (Eckhaus boundary) of the spatially periodic waves is given by $\mathcal{D}(q)=0$ and is denoted by the dashed lines in Figs. 1(a)–1(c). From Eqs. (5), (9), and (10) one can see that if the imaginary parts of the various parameters are zero, then the neutral-stability and Eckhaus curves are symmetric around $q=0$. Even if the neutral curve has multiple minima, and consequently the band of stable wave numbers is separated into subbands, these subbands merge for large forcing. This can be seen directly from Eqs. (9) and (10) by considering the limit $S\to\infty$. For $c_i=0$ the leading-order term $\{-4(3c_ifq+c^*d)|n|^2\}S^6$ of $D(q)$ is positive since $c_r<0$ and $d_r>0$. Thus $\mathcal{D}$ becomes positive for large S, independent of the other coefficients, since $\tau>0$ for large S.

The same consideration shows that for general coefficients, i.e., for $c_i\neq 0$ and $f\neq 0$, the diffusion coefficient $\mathcal{D}$ always becomes negative for large S for some range of q. For the parameters chosen in Figs. 1(a)–1(c), this occurs for $q>0$. Thus for $a_i=-0.7$ one obtains two stable subbands which do not merge for large forcing. With increasing a_i two additional resonances arise for smaller q, leading to a quite flat neutral curve. Strikingly, the left stable subband splits up into two bands leading to three separate bands right at onset [Fig. 1(b)]. Upon a further increase to $a_i=0.5$ the large-q subband merges with the central one for small forcing. For

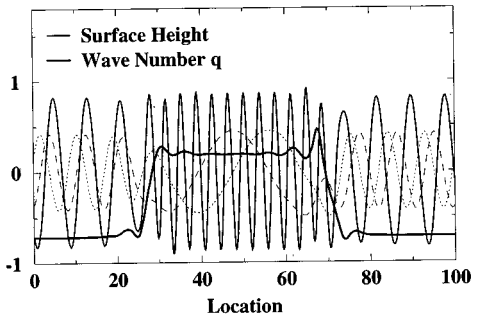

FIG. 2. A typical domain structure arising from Eqs. (2) and (3) for $a_r=-0.5+0.5i$, $b=1.3$, $d=0.1$, $v=1+0.2i$, $f=-3$, $c=-1-0.5i$, $n=-3+2i$ [cf. Fig. 1(c)]. The thin solid line gives $\mathrm{Re}(e^{iq_cx}(A+B))$, with $q_c=1.5$. The short and long dashed lines indicate the real and imaginary parts of A, respectively.

large forcing they remain separated. The merging of the central band with the left band occurs now only at larger values of the forcing b [Fig. 1(c)].

IV. NUMERICAL SIMULATIONS

To show that the complex stability regions shown in Figs. 1(a)–1(c) indeed lead to stable domain structures consisting of domains with large and small wave numbers, we solved Eqs. (2) and (3) with periodic boundary conditions numerically using a finite-difference code with Crank-Nicholson time-stepping. A typical domain structure is shown in Fig. 2. It was obtained for parameter values that correspond to Fig. 1(c) (with $b=1.3$) and the location of this domain structure in (q,b) space is indicated by the dotted line on that figure. The domain structure itself consists of a region with $q\approx 0.19$ in the center of the figure and $q\approx -0.72$ at the boundaries (thick line). These wave numbers correspond to the two Eckhaus-stable wells for the selected parameter values. Between the two domains there is a sharp transition. This domain structure is numerically stable. The thin line gives $\mathrm{Re}(\exp(iq_cx)\{A+B\})$ with $q_c=1.5$, and is intended to give an impression of a typical surface deformation in this regime. The broken lines give the real and imaginary part of A. The dots in Fig. 1(c) give the wave number distribution of the solution shown in Fig. 2. The higher density of dots near $q=-0.7$ and 0.2 shows that over most of the system the local wave number is within one of the two stable regimes.

From an experimental point of view an important question is how one obtains these domain structures. Clearly, an adiabatic increase of the periodic forcing in the frequency regime in which the neutral curve has two different minima will not be successful since the emerging pattern will always be periodic with the wave number corresponding to the deeper minimum. Instead, one has to increase the forcing suddenly from values below threshold to a value for which the wavenumber band consists of at least two subbands. Even then one may still predominantly obtain patterns with the wave number corresponding to the deeper minimum. Alternatively, one can change the forcing frequency at a fixed supercritical forcing amplitude in the regime in which the stable band is split. The change in frequency shifts the band of stable wave numbers, and eventually the initially stable wave becomes unstable. If its wave number hits the part of

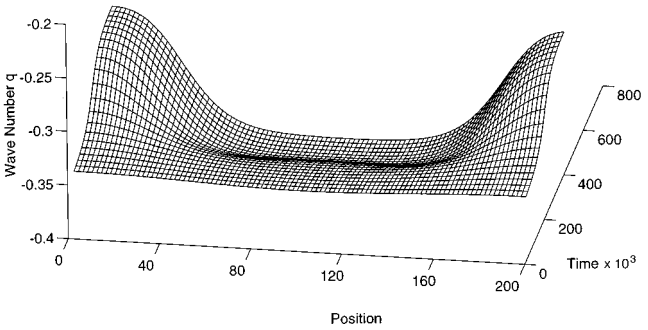

FIG. 3. Temporal evolution of the local wave number. The initial wave number is $q\approx -0.34$. The forcing is $b=1.7$. The remaining parameters are $a=-0.5+0.1i$, $d=0.1$, $v=1+0.2i$, $c=-1-0.5i$, $n=-3+2i$, and $f=-3$ [cf. Fig. 1(b)].

the stability boundary which faces the other subband [as marked by the open square in Fig. 1(c)] it is expected that the instability will not lead to a phase slip but to domain structures.

The best approach is presumably to prepare a periodic pattern in the single-well regime, i.e. for $M<M_c$, with the wave number (i.e. the frequency) chosen such that it falls into the unstable region between two subbands once the dc magnetic field is suddenly increased to reach $M>M_c$. The numerical result of such a protocol is shown in Fig. 3. This gives the space-time diagram for the local wave number, and clearly shows how the pattern separates into domains with different wave numbers after a jump from $v_r>0$ to $v_r<0$, which renders the initial wave number in the region of instability between the left two subbands of Fig. 1(b) ($b=1.7$). In the simulation the initial condition was perturbed with a long-wave modulation of the wave number in order to trigger the long-wave Eckhaus instability. Note that the initial condition was placed very close to the top of the hump of the Eckhaus curve in order to insure that the fastest growing mode has a long wavelength leading to a single low-wave number domain. Thus the diffusion coefficient is only weakly negative, and the evolution is extremely slow.

A second simulation is shown in Fig. 4. Here the initial

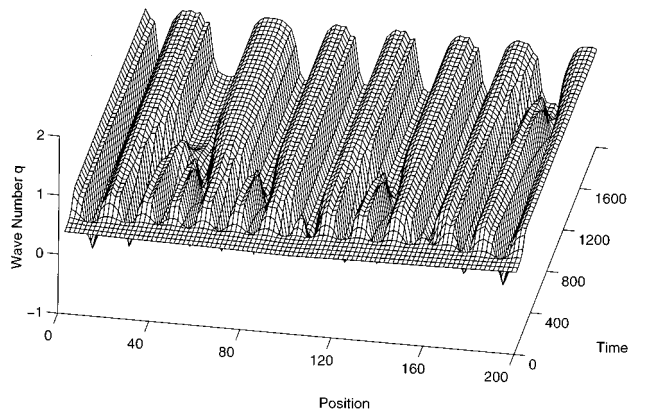

FIG. 4. Temporal evolution of the local wave number. The initial wave number is $q=0.28$, and $b=2$ [cf. Fig. 1(b)]. The remaining parameters are as in Fig. 3. The fastest growing mode has a short wavelength, and leads to a large number of small domains which then undergo a coarsening process.

wave number is $q=0.28$ and $b=2$, i.e., the wave number falls between two subbands which are completely separated from each other. The evolution of the wave number is strikingly different from Fig. 3. Although the initial perturbation was the same as in Fig. 3, large oscillations in the wave number arise after a short time. Apparently, in this regime the fastest growing mode has a short wavelength. Presumably, this represents the usual shift to shorter wavelengths when the Eckhaus boundary is exceeded substantially. In principle it could, however, also indicate an additional short-wavelength instability not captured in the phase equation (6).

Figure 4 shows that the sideband instability can lead — at least initially — to quite complex arrays of domains. As can be seen in that figure, the domains evolve slowly over time in a coarsening process in which adjacent domain walls (fronts) annihilate each other, thereby reducing the number of domains. Thus the interaction between the domain walls plays a crucial role in determining whether the coarsening will continue and eventually will lead to a state consisting only of two large domains of different wave numbers, or whether the coarsening comes to a halt leading to a complex structure like that shown in Fig. 4 at large times. The latter is expected if the interaction between the domain walls is oscillatory in space. This would allow a discrete set of equilibrium distances between the domain walls [14]. Oscillations in the wave number — as apparent in Fig. 2 — suggest that the interaction could indeed be oscillatory. A detailed study of this issue is, however, beyond the scope of this paper. Here we will present only simulations of a simpler model which can be derived from Eqs. (2) and (3) in a special case.

The locking of adjacent fronts in the wave number has been discussed in detail within the framework of a single Ginzburg-Landau equation with fourth-order spatial derivatives, which models a neutral curve with two equal minima [15,17,12,13],

$$\frac{\partial \mathcal{A}}{\partial \tilde{T}} = D_2 \frac{\partial^2 \mathcal{A}}{\partial \tilde{X}^2} - D_4 \frac{\partial^4 \mathcal{A}}{\partial \tilde{X}^4} + \Sigma \mathcal{A} - \Gamma |\mathcal{A}|^2 \mathcal{A}. \qquad (11)$$

Such a neutral curve is obtained for Eqs. (2) and (3) in the special case where $v=0$ and $f=0$. If in addition the two minima are not too deep, the Ginzburg-Landau equation (11) can be derived from Eqs. (2) and (3) near threshold, and one obtains $D_2 = d_r + a_i d_i / a_r$, $D_4 = -d_i^2 |a|^2/(2a_r^3)$, $\Sigma = -|a|(b-|a|)/a_r$, and $\Gamma = (n_r a_r + n_i a_i)/(2a_r)$ [6]. The complex amplitude $\mathcal{A}$ is proportional to the amplitudes A and B of the left- and right-traveling wave components of the standing wave $|A|=|B|$. The slowness of the slow scales $\tilde{X}$ and $\tilde{T}$ is related to the distance from threshold. Equation (11) has also been studied in the context of two-dimensional zigzag patterns. There the locking discussed below has been identified previously [15–17]. As discussed in [13], no locking is possible within the phase equation (6). Locking can therefore arise only in regimes in which the phase equation breaks down, as is, for instance, the case very close to threshold. Thus, Eq. (11) is expected to capture some aspects of the dynamics of fronts in Eqs. (2) and (3).

Numerical simulations of Eq. (11) yield a surprisingly rich behavior for small domain structures which consist only of two domains. This is discussed in detail in [13]. Here our interest is in the behavior of long systems containing many domains. In particular, we are interested in the interaction between adjacent domain walls. In [13] a discrete set of solutions has been found, in which the fronts are locked into each other due to the oscillatory behavior of the local wave number similar to that of the structure shown in Fig. 2 (see also [17]). The oscillations lead to a discretization of the allowed domain widths, such that the domains can be characterized by the number of oscillations contained in them. They disappear when D_2 is raised from negative values toward 0. The dependence of the range of existence of a domain on the number of oscillations has been studied in [13] for domains ranging from 1 to 9 extrema in the wave number. It was found that among these domains those with five extrema exist over the largest range of D_2.

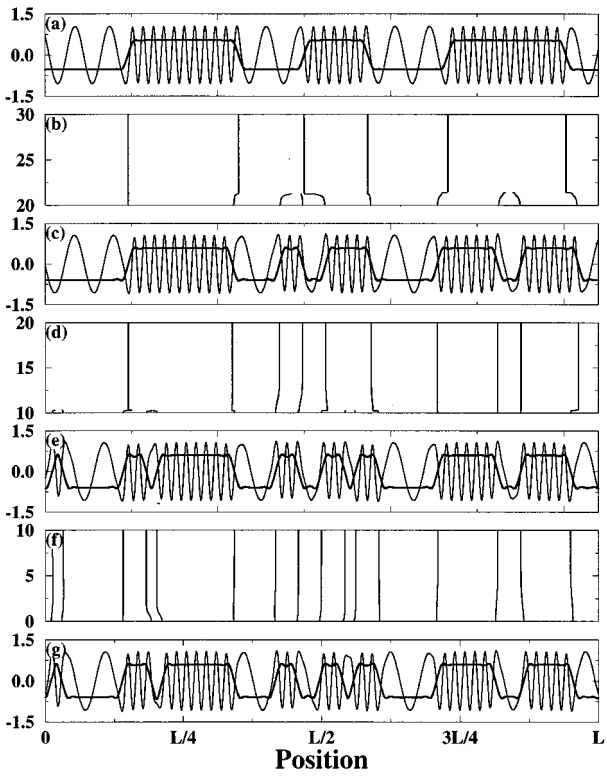

FIG. 5. Simulations of Eq. (11). Positions of domain walls as they evolve, and the domain structures observed at various times. Parts (a), (c), (e), and (g) show the wave number (thick line) and $\mathrm{Re}(\mathcal{A}e^{iq_0 x})$ (thin line), while (b), (d), and (f) plot the positions of zeros of the wave number as a function of time (running upward). For all figures, $\Sigma=1.0$, $D_4=1$, and $L=217.36$, and for (a)–(c) $D_2=-0.72$, (d) and (e) $D_2=-0.7$; and (f) and (g) $D_2=-0.58$. The times indicated in (b), (d), and (f) are time/10 000.

In Figs. 5(g)–5(a) we present the typical evolution of a large array of domains for periodic boundary conditions when the coefficient D_2 is increased from negative values. The initial condition [Fig. 5(g)] consists of an arbitrarily chosen sequence of domains of different sizes. Figure 5(f) shows the temporal evolution of the zero crossings of the wave number at fixed $D=0.72$; clearly, domains that do not have the appropriate width become either wider or narrower in order to lock the domain walls at an appropriate distance. The resulting state [Fig. 5(e)] is stable. In analogy to the analysis of spatial chaos in a Ginzburg-Landau equation with

real amplitude [14], it is expected that in very long arrays of the type shown in Fig. 5(d) the sequences of domain lengths can be chaotic [16,17].

If D_2 is changed from $D_2=-0.72$ to $D_2=-0.7$, states which have only one extremum between adjacent walls cease to exist, and the adjacent domain walls annihilate each other. Such a situation is shown in the sequence Figs. 5(e)–5(c). The single-extremum states disappear very soon after the control parameter is changed. The remaining states then reorder themselves to retain their desired spacing. A similar process is observed in the sequence Fig. 5(c)–5(a) when the control parameter is changed to $D_2=-0.58$, a value at which the three-extrema states no longer exist. Again, the domain walls annihilate each other and a stable state consisting only of very wide domains is reached. In the numerical simulations such states with more than nine extrema were not found to be stable. On an exponentially long time scale the state depicted in Fig.5(a) is therefore expected to coarsen to a state with only one domain with large wave number and one domain with small wave number.

We expect that Eqs. (2) and (3) possess stable solutions similar to those shown in Fig. 5, which consist of arrays of domains of different widths and which undergo coarsening transitions when parameters are changed. The main difference between Eqs. (11) and (2) and (3) seems to be that, in the general case, Eqs. (2) and (3) are not even in the wave number. Therefore domains with positive and negative wave numbers are not equivalent. In preliminary simulations of Eqs. (2) and (3) for parameters as in Fig. 1 ($1<b<2$), domains with negative wave numbers appeared to be less stable than those with positive wave numbers, which often lead to a merging of the latter. There seemed to be only a weak locking of the respective fronts, if any. For small asymmetry, however, the dynamics as shown in Fig. 5 should still be possible in the full equations. The effect of an asymmetry can also be studied by simulations of Eq. (11) with an additional third derivative [33].

V. CONCLUSION

In this paper we investigated the stability of parametrically driven waves in systems in which the dispersion relation for unforced waves is nonmonotonic. We studied coupled Ginzburg-Landau equations which are valid for small amplitudes and in the vicinity of the inflection point in the dispersion relation. As expected the neutral curves for the excitation of the waves exhibit multiple minima in this regime, and consequently the band of stable wave numbers is split up into three subbands. Numerical simulations show that under these conditions patterns consisting of an array of domains with different wave numbers can be stable. Our results suggest that such domain structures should be readily accessible experimentally. Particularly suitable experiments on surface waves in ferrofluids appear in the presence of static and time-periodic magnetic fields. There the nonmonotonic dispersion relation is a precursor of the Rosensweig instability [24,25]. Analogous experiments with conducting or dielectric fluids in the presence of the corresponding electric fields are expected to give similar results [26–29].

It has been pointed out previously [6,9] that domain structures are also likely to occur if a parametric forcing is applied to waves which are Benjamin-Feir unstable [34] in the absence of forcing. This can be seen from Eq. (9). In the limit of large amplitudes the diffusion coefficient becomes negative in the band center if $c_r d_r + c_i d_i > 0$, which is the condition for Benjamin-Feir instability of the unforced waves [35]. This implies that either the parametrically forced waves become unstable at all wave numbers, or that the stable band has split into subbands. In the latter case domain structures should arise.

An interesting open question concerns the stability of domain structures in two dimensions. If the wave numbers in the different domains differ only in their orientation but not in their magnitude, one obtains zigzag structures. In isotropic systems they arise generically due to the annular shape of the range of stable wave numbers. In axially anisotropic systems they appear when the instability of the structureless state is to rolls or waves oblique to the preferred direction. The stability of zigzag structures has been studied in some detail [13,36], in particular in systems with axial anisotropy [15,17].

Neutral stability surfaces for parametrically driven waves in two-dimensional anisotropic systems were studied in some detail in [32]. There, interesting situations with multiple minima at different orientations as well as different magnitudes of the wave number have been found, suggesting the possibility of a patchwork of two-dimensional domains in which the wave numbers differ not only in their orientation but also in their magnitude. Can such structures be stable? Some impression can be gained from a simulation presented in [37] (see also [11]). Figure. 3(b) of [37] shows the result of a two-dimensional simulation of the coupled Ginzburg-Landau equations for parametrically driven waves (with normal dispersion) in an anisotropic system. The pattern shown is clearly characterized by domains or patches with large and small wavelengths. Although the authors attribute the result to a Benjamin-Feir instability of the waves, i.e., a situation in which waves of *all* wave numbers become unstable, a comparison with Eq. (9) shows that for the parameters chosen in that simulation the stable band is split into two subbands with the critical wave number $q=0$ lying in the unstable region between. Only the stability of that latter wave number was studied in [37]. A better understanding of such complex two-dimensional domain structures is clearly desirable.

Finally, an extension to traveling waves is also of interest. So far, domain structures of traveling waves have been investigated only within a suitable phase equation [38]. The possibility of a locking of the domain walls has, however, not been addressed.

ACKNOWLEDGMENTS

HR gratefully acknowledges stimulating discussions with I. Rehberg and V. Steinberg. This work was supported by the DOE through Grant No. DE-FG02-92ER14303, and by an equipment grant from the NSF (No. DMS-9304397). D.R. was supported by the U.S. Department of Energy, Contract No. DE-FG05-95ER14566, and also in part by the Supercomputer Computations Research Institute, which is partially funded by the U.S. Department of Energy, Contract No. DE-FC05-85ER25000.

[1] M. Cross and P. Hohenberg, Rev. Mod. Phys. **65**, 851 (1993).
[2] Y. Pomeau and P. Manneville, J. Phys. Lett. (Paris) **23**, L609 (1979).
[3] W. Eckhaus, *Studies in Nonlinear Stability Theory* (Springer, New York, 1965).
[4] L. Kramer and W. Zimmermann, Physica D **16**, 221 (1985).
[5] H. Brand and R. Deissler, Phys. Rev. Lett. **63**, 508 (1989).
[6] H. Riecke, Europhys. Lett. **11**, 213 (1990).
[7] R. Deissler, Y. Lee, and H. Brand, Phys. Rev. A **42**, 2101 (1990).
[8] H. Brand and R. Deissler, Phys. Rev. A **41**, 5478 (1990).
[9] H. Riecke, in *Nonlinear Evolution of Spatio-Temporal Structures in Dissipative Continuous Systems*, edited by F. Busse and L. Kramer (Plenum, New York, 1990), pp. 437–444.
[10] J. Hegseth, J. Vince, M. Dubois, and P. Bergé, Europhys. Lett. **17**, 413 (1992).
[11] S. Residori *et al.*, Phys. Rev. Lett. **76**, 1063 (1996).
[12] D. Raitt and H. Riecke, in *Spatiotemporal Patterns in Nonequilibrium Complex Systems, Santa Fe Institute*, edited by P. Cladis and P. Palffy-Muhoray (Addison-Wesley, Reading, MA, 1995), pp. 255–264.
[13] D. Raitt and H. Riecke, Physica D **82**, 79 (1995).
[14] P. Coullet, C. Elphick, and D. Repaux, Phys. Rev. Lett. **58**, 431 (1987).
[15] W. Pesch and L. Kramer, Z. Phys. B **63**, 121 (1986).
[16] E. Bodenschatz, W. Zimmermann, and L. Kramer, J. Phys. (Paris) **49**, 1875 (1988).
[17] E. Bodenschatz *et al.*, in *The Geometry of Non-Equilibrium*, edited by P. Coullet and P. Huerre (Plenum, New York, 1990), p. 111.
[18] F. Busse and F. Finocchi, Phys. Earth Planetary Interiors **80**, 13 (1993).
[19] R. Tagg, W. Edwards, and H. Swinney, Phys. Rev. A **42**, 831 (1990).
[20] S. Tennakoon, C. Andereck, J. Hegseth, and H. Riecke, Phys. Rev. E (unpublished).
[21] I. Rehberg *et al.*, Phys. Rev. Lett. **61**, 2449 (1988).
[22] M. de la Torre-Juarez and I. Rehberg, Phys. Rev. A **42**, 2096 (1990).
[23] T. Mahr, A. Groisman, and I. Rehberg, J. Magn. Magn. Mater. (to be published).
[24] R. Rosensweig, *Ferrohydrodynamics* (Cambridge University Press, Cambridge, 1985).
[25] R. Rosensweig, Ann. Rev. Fluid Mech. **19**, 437 (1987).
[26] G. Taylor and A. McEwan, J. Fluid Mech. **22**, 1 (1965).
[27] J. He, N. Miskovsky, P. Cutler, and M. Chung, J. Appl. Phys. **68**, 1475 (1990).
[28] G. de Surgy, J. Chabrerie, O. Denoux, and J. Wesfreid, J. Phys. II **3**, 1201 (1993).
[29] A. Elhefnawy, Physica A **297**, 561 (1994).
[30] H. Riecke, J. Crawford, and E. Knobloch, Phys. Rev. Lett. **61**, 1942 (1988).
[31] D. Walgraef, Europhys. Lett. **7**, 485 (1988).
[32] H. Riecke, M. Silber, and L. Kramer, Phys. Rev. E **49**, 4100 (1994).
[33] M. Proctor, Phys. Fluids A **3**, 299 (1991).
[34] T. Benjamin and J. Feir, J. Fluid Mech. **27**, 417 (1967).
[35] J. Stuart and R. DiPrima, Proc. R. Soc. London Ser. A **362**, 27 (1978).
[36] B. Malomed, A. Nepomnyashchy, and M. Tribelsky, Phys. Rev. A **42**, 7244 (1990).
[37] P. Coullet, K. Emilsson, and D. Walgraef, Physica D **61**, 132 (1992).
[38] H. Brand and R. Deissler, Phys. Rev. A **46**, 888 (1992).